Osteoporos Int
DOI 10.1007/s00198-008-0820-y

ORIGINAL ARTICLE

Comparison of QCT-derived and DXA-derived areal bone mineral density and *T* scores

B. C. C. Khoo · K. Brown · C. Cann · K. Zhu · S. Henzell · V. Low · S. Gustafsson · R. I. Price · R. L. Prince

Received: 23 May 2008 / Accepted: 3 November 2008

Abstract
Summary Two-dimensional areal bone mineral density (aBMD) of the proximal femur measured by three-dimensional quantitative computed tomography (QCT) in 91 elderly women was compared to dual-energy X-ray absorptiometry (DXA) aBMD results measured in the same patients. The measurements were highly correlated, though QCT aBMD values were marginally lower in absolute units. Transformation of the QCT aBMD values to *T* score values using National Health and Nutrition Examination Survey (NHANES) DXA-derived reference data improved agreement and clinical utility.
Introduction World Health Organization guidelines promulgate aBMD (g cm^{-2}) measurement of the proximal femur for the diagnosis of bone fragility. In recent years, there has been increasing interest in QCT to facilitate understanding of three-dimensional bone structure and strength.
Objective To assist in comparison of QCT-derived data with DXA aBMD results, a technique for deriving aBMD from QCT measurements has been developed.
Methods To test the validity of the QCT method, 91 elderly females were scanned on both DXA and CT scanners. QCT-derived DXA equivalent aBMD (QCT_{DXA} aBMD) was calculated using CTXA Hip™ software (Mindways Software Inc., Austin, TX, USA) and compared to DXA-derived aBMD results.
Results Test retest analysis indicated lower root mean square (RMS) errors for CTXA; *F* test between CTXA and DXA was significantly different at femoral neck (FN) and trochanter (TR) ($p<0.05$). QCT underestimates DXA values by 0.02±0.05 g cm^{-2} (total hip, TH), 0.01±0.04 g cm^{-2} (FN), 0.03±0.07 g cm^{-2} (inter-trochanter, IT), and 0.02±0.05 g cm^{-2} (TR). The RMS errors (standard error of estimate) between QCT and DXA *T* scores for TH, FN, IT, and TR were 0.36, 0.40, 0.39, and 0.49, respectively.
Conclusions This study shows that results from QCT aBMD appropriately adjusted can be evaluated against NHANES reference data to diagnose osteoporosis.

Keywords Areal bone mineral density · Dual-energy X-ray absorptiometry · Femoral neck · Proximal femur · Quantitative computer tomography · Total hip · *T* scores

B. C. C. Khoo · R. I. Price
Medical Technology and Physics, Sir Charles Gairdner Hospital, Perth, Australia

K. Brown · C. Cann
Mindways Software,
Austin, TX, USA

K. Zhu · S. Henzell · S. Gustafsson · R. L. Prince (✉)
Department of Endocrinology and Diabetes,
Sir Charles Gairdner Hospital,
Perth, Western Australia
e-mail: rlprince@cyllene.uwa.edu.au

K. Zhu · R. L. Prince
School of Medicine and Pharmacology, University of Western Australia,
Perth, Australia

V. Low
Department of Radiology, Sir Charles Gairdner Hospital,
Perth, Australia

Introduction

Areal bone mineral density (aBMD in grams per square centimeter) estimates for the proximal femur using dual-energy X-ray absorptiometry (DXA) are currently considered

Published online: 24 December 2008

the gold standard for making a diagnosis of osteoporosis in an individual patient [1] and more recently in predicting fracture risk [2]. However, structural information can be derived from quantitative computer tomography (QCT)-based methods that are difficult to obtain using DXA methods. For example, QCT studies of the proximal femur have shown a strong relationship between bone mass and its distribution and bone strength [3]. In particular, geometric measurements derived from QCT may represent in vivo strength better than DXA BMD [4].

To date, there are limited QCT bone structure data from prospective clinical studies available to form a context for interpretation of these measurements in terms of fracture risk. In this study, we compare DXA equivalent proximal femoral aBMD derived from a new projection QCT method with the aBMD derived from conventional DXA in the same patient population.

Methods

Patients

Reproducibility studies Each subject was scanned twice on the same day with each subject getting off and on the computed tomography (CT) or DXA table and being repositioned prior to acquisition of the second scan.

QCT DXA comparison

Mindways dataset Comparison of QCT aBMD values and DXA aBMD values to derive the QCT_{DXA} aBMD values reported by Mindways software was obtained by the addition of a QCT hip study to patients having a DXA hip study for clinical purposes. Subjects provided informed consent with institutional review board oversight.

Perth dataset The comparison of DXA- and QCT-derived aBMD was undertaken on patients recruited from the CAIFOS Age-Related Extension Study cohort study, a community-based 5-year random control trial of the effect of calcium supplementation on fracture risk in the elderly [5] extended as an epidemiological study of musculoskeletal and cardiovascular disease in elderly women. All women were living independently in the community; one half had sustained at least one fracture. Exclusion criteria include skeletal disease other than osteoporosis. Subjects provided informed consent with institutional review board oversight.

QCT analysis

To allow data obtained on different CT scanners to be standardized, prior to the clinical use of machines, eight to ten images of the Mindways quality assurance (QA) phantom were acquired using the same technique as for subject scans. QCT PRO™ QA analysis software (Mindways Software Inc., Austin, TX, USA) was used to determine the individual CT scanner performance characteristics. Results were referenced to the appropriate CT scanner QA results and the QA phantom was scanned at regular intervals to monitor scanner performance.

Subjects were positioned supine on the CT scanner table, lying on top of a QCT PRO™ calibration phantom and bolus bag so that the calibration phantom extended from the lumbar vertebrae to below the lesser trochanter (TR). The QCT PRO™ calibration phantom is based on an original QCT calibration system developed at the University of California, San Francisco [6]. The patient was positioned so that the pelvis was as straight as possible, the knees flat on the scanner table with legs straight, heels out, and toes pointed inward. Subjects were instructed to remain still and breathe normally during the study. The right hip was analyzed unless pathology prevented this. An anterior–posterior computed radiograph was obtained by the scanner from the iliac crest to mid-thigh.

The reproducibility studies were undertaken on a GE NXi CT (GE Medical Systems, Madison, WI, USA) scanner. The Mindways data were acquired on Philips SR4000 (Philips Medical Systems, Andover, MA, USA) and GE ProSpeed (GE Medical Systems, Madison, WI, USA) scanners. Patients were scanned at 120 kVp with exposure based on subject height and weight, from a lookup table supplied with the CTXA Hip™ software. A contiguous series of CT images were acquired with a 3-mm slice thickness and with 3-mm spacing between images. Typically, 40 images were obtained and the CT images were reconstructed using a standard abdomen reconstruction method. Perth studies were undertaken on a Phillips Brilliance 64 slice spiral QCT scanner. Scans were acquired at 120 kVp, 150 mA s, 1-mm slice thickness, and a pitch of 1. Effective dose from this scan protocol was 2.9 mSv [7].

The QCT-derived aBMD was determined using Mindways CTXA Hip software version 4.1 according to the directions provided by the manufacturer (Mindways Software Inc.). Analysis was performed by positioning a square region of interest (ROI) centered over the femoral neck (FN) as identified on the axial images and a volumetric region of interest containing the proximal femur extracted from the CT image dataset. Segmentation of bone from surrounding soft tissue was performed using an adaptive algorithm with a base threshold of 120 mg cm^{-3} to identify the bone surface. This resulted in a dataset of voxels identified as "bone," all contained within the envelope formed by outer cortex of the proximal femur. This 3D dataset of bone voxels was

then rotated so that the femoral shaft was vertical in the coronal and sagittal planes with the femoral neck axis in the coronal plane. From the rotated 3D data, a 2D image similar to a DXA image was generated by summing all the bone voxels along lines perpendicular to the coronal plane. Each pixel of the resulting image represented the mass of mineral summed along that line and was further characterized by a known pixel area and a total volume of bone along the line. Regions of interest representing those commonly used for DXA analysis (total hip (TH), FN, inter-trochanter (IT), and TR) were identified automatically on the projected image by the software. The ROIs defined by the software are substantially similar to those used in Hologic DXA devices. The automatically identified ROIs were visually checked to verify that the lower extent of the inter-trochanter ROI was set at the lower junction of the lesser trochanter and the femoral shaft and that the femoral neck axis and femoral neck ROI position and size were appropriate. The ROIs were adjusted by the operator as required. Results for aBMD (g cm^{-2}) were reported in terms of equivalent calibrated aqueous potassium phosphate density and were stored in the QCT PRO™ database for export as text files.

DXA scanning and analysis

The reproducibility studies were undertaken on a Hologic QDR 2000 scanner; scans for the Perth dataset were performed on a Discovery A scanner. DXA scans for the Mindways dataset were acquired on Hologic 4500A scanners. DXA scanners were maintained according to the manufacturer's recommendations, including the performance of daily calibrations for quality control (QC) using the Hologic three-dimensional spine phantom. Data were acquired in hip scan array mode from the right hip, unless pathology prevented this; the effective dose from a typical scan was 6 μSv. The scan was analyzed according to the manufacturer's instructions using Hologic software version 12.6 (Hologic, Boston, MA, USA) and the results were reported in terms of grams per square centimeter hydroxyapatite (HA) equivalent.

Data analysis

All results are mean (SD); all p values are estimated from two-tailed testing. The QCT-based DXA equivalent T score (QCT_{DXA} T score) was calculated as follows:

$$QCT\_T_{score} = \left(\frac{aBMD_{QCT} - aBMD_{yn}}{SD_{yn}}\right) \quad (1)$$

Where $aBMD_{yn}$ is the mean aBMD of the NHANES III (National Health and Nutrition Examination Survey III) young-adult normal reference population; $aBMD_{QCT}$ is the QCT_{DXA} aBMD, and SD_{yn} is the standard deviation of the aBMD distribution of the NHANES III young female reference population [8] (TH 0.942±0.122 (mean±SD [g cm^{-2}]), FN 0.849±0.111, IT 1.086±0.155, TR 0.703±0.101).

Results

In vivo short-term precision

The QCT reproducibility study was undertaken in 24 patients, 15 females and nine males, age 61.4 (11.2) years [mean (SD)]. The DXA reproducibility study was undertaken in 71 female patients, age 50.5 (6.5) years [9]. The results of the analyses are shown in Table 1. The RMS errors were typically lower for CTXA compared to DXA. F tests between CTXA and DXA were significantly different at FN and TR ($p<0.05$).

Comparison of DXA and QCT

The 91 women who undertook this study had a mean age of 82.8 (2.5) years, a mean height of 157.4 (6.1) cm, a mean weight of 64.2 (10.7) kg, and a mean BMI of 25.9 (3.9) kg m^{-2}.

The Mindways regression equations used to convert the QCT-derived aBMD results in grams per square centimeter aqueous potassium phosphate density to DXA equivalent aBMD in grams per square centimeter HA equivalent are reported in Table 2.

The analytical approach to the Perth dataset is shown in Fig. 1, with data shown in Table 3. The DXA- and QCT-

Table 1 Short-term reproducibility studies

	QCT mean (SD) values	QCT RMS error	DXA mean (SD) values	DXA RMS error
Femoral neck (g cm^{-2})	0.69 (0.09)	0.008*	0.76 (0.10)	0.013
Total hip (g cm^{-2})	0.82 (0.12)	0.008	0.88 (0.11)	0.010
Inter-trochanter (g cm^{-2})	0.98 (0.16)	0.014	1.03 (0.13)	0.018
Trochanter (g cm^{-2})	0.64 (0.12)	0.007*	0.70 (0.10)	0.010

*$p<0.05$ compared to DXA precision

Table 2 Correlation between DXA aBMD and QCT aBMD

Region	Transformation equation	R^2
Femoral neck	DXA=(QCT+0.004)/0.888	0.89
Total hip	DXA=(QCT+0.106)/1.006	0.93
Inter-trochanter	DXA=(QCT+0.101)/0.994	0.91
Trochanter	DXA=(QCT+0.076)/0.985	0.91

Transformation equations obtained from the Mindways dataset

derived area and mineral mass data are quite different which is not surprising given the differences in the techniques and standards. Using the conversion equations reported in Table 2 considerably improved the similarity to the Hologic DXA data. Bland Altman plots using these converted data for the four sites of the proximal femur are shown in Fig. 2. The largest difference was found at the IT (0.03±0.07 g cm^{-2}) while the smallest difference was at the FN (0.01±0.04 g cm^{-2}). These plots confirm that QCT-transformed aBMD was slightly lower than the corresponding DXA-derived aBMD, with trends significant for TH and IT (p=0.03; Fig. 2). The RMS errors between QCT_{DXA} aBMD and DXA aBMD were 0.04 g cm^{-2} (TH), 0.04 g cm^{-2} (FN), 0.06 g cm^{-2} (IT), and 0.05 g cm^{-2} (TR).

The QCT_{DXA} aBMD and DXA-derived aBMD data were then transformed to an equivalent T score using the NHANES III reference data. Figure 3 shows the linear regression plots of QCT-transformed T scores and the DXA-derived T scores. R^2 values range between 0.84 and 0.88; again, there is no systematic or individual deviation from the linear conversion model. The RMS error for TH, FN, IT, and TR were 0.36, 0.40, 0.39, and 0.49, respectively. A complete set of conversion equations to derive DXA T scores from QCT-transformed aBMD values is provided in the "Appendix."

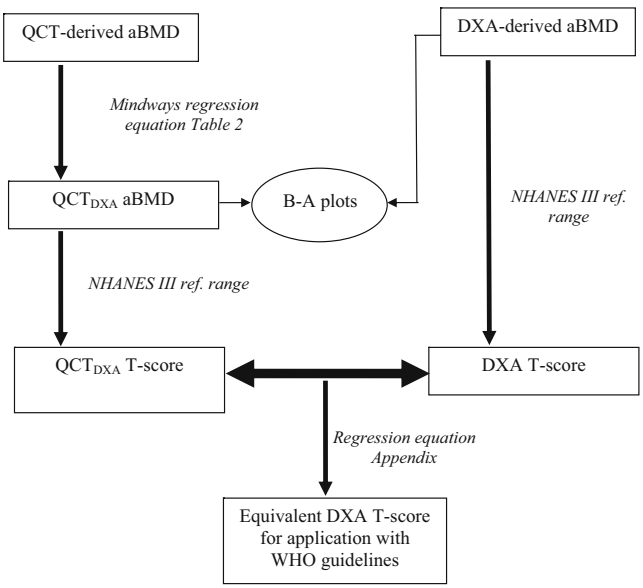

Fig. 1 Summary flow chart on the Perth acquired data, indicating the process and terms defined in the text. Each of the four proximal femur sites (TH, FN, IT, TR) were analyzed in the same way

Discussion

The results of our study showed that aBMD results obtained using the QCT software are highly correlated with results obtained from a planar DXA device. Indeed, the results obtained in our study are similar to the relationship seen between the Hologic and GE-Lunar DXA systems where a correlation of R=0.92 and RMS error of 0.05 g cm^{-2} for the FN ROI over the same aBMD range in similar populations has been reported [10, 11]. However, the QCT_{DXA} aBMD values were lower than the corresponding DXA-derived aBMD. The RMS error for the FN between Hologic and GE-Lunar was 0.05 g cm^{-2} [10], similar to between Hologic and QCT (0.04 g cm^{-2}) for the corresponding site. Similar biases in aBMD estimates between bone densitometers from different manufacturers of the same magnitude reported in this study have been observed in comparison studies of DXA devices from Hologic, GE-Lunar, and Norland [10, 11]. The aBMD differences between GE-Lunar (Prodigy) and Hologic (Delphi) at the FN and TH were 0.15 and 0.07 gcm^{-2} (GE-Lunar–Hologic), respectively [12]. GE-Lunar aBMD at both FN and TH sites was consistently higher compared to Hologic. In a similar comparison, differences between Hologic and QCT aBMD in this study were 0.02 and 0.01 gcm^{-2} (Hologic–QCT) for TH and FN sites, respectively.

One cause of the differences between QCT_{DXA} aBMD and DXA-derived aBMD relates to the calibration phantoms used [13]. The Hologic DXA scanner uses a spine phantom which is made of solid hydroxyapatite standard for its QC and a filter wheel for its calibration. QCT uses liquid potassium phosphate (K_2HPO_4) as a mineral standard. Although the mean HA and K_2HPO_4 calibration standards are similar in the trabecular aBMD region, there are slight differences in the calibration slopes, with a propensity for K_2HPO_4 equivalent densities to be slightly lower than corresponding HA equivalent densities. The difference is more pronounced when working at higher densities. Therefore, it is not surprising that QCT-derived mineral mass (BMC) at all corresponding sites of the proximal femur was significantly lower compared to DXA values (Table 3). In addition, the manner in which aBMD is calculated in DXA and QCT is fundamentally different. DXA technique is constrained by two equations in a three-compartment object, and, to overcome this additional

Table 3 Results of the Perth comparison of DXA and QCT techniques

	Femoral neck	Total hip	Inter-trochanter	Trochanter
DXA mass (g)	3.40 (0.64)	27.79 (5.45)	17.57 (3.58)	6.83 (1.71)
QCT mass (g)	2.93 (0.56)*	20.74 (3.89)*	12.60 (2.37)*	5.18 (1.32)*
DXA area (cm^2)	5.13 (0.41)	35.61 (3.12)	19.37 (2.34)	11.12 (1.54)
QCT area (cm^2)	5.10 (0.42)	31.84 (2.91)*	16.39 (1.90)*	10.19 (1.31)*
DXA aBMD (g cm^{-2})	0.66 (0.11)	0.78 (0.14)	0.91 (0.17)	0.61 (0.13)
QCT aBMD (g cm^{-2})	0.57 (0.10)*	0.65 (0.13)*	0.77 (0.15)*	0.51 (0.13)*
QCT_{DXA} aBMD (g cm^{-2})	0.65 (0.11)**	0.76 (0.13)*	0.88 (0.15)*	0.60 (0.13)*
DXA *T* score (units)	−1.69 (0.95)	−1.32 (1.12)	−1.13 (1.07)	−0.89 (1.28)
QCT *T* score (units)	−1.79 (0.99)**	−1.52 (1.03)*	−1.32 (0.97)*	−1.05 (1.27)*

Results are mean (SD). QCT_{DXA} aBMD results are QCT aBMD results transformed using the equations in Table 2
*$p<0.005$; **$p=0.02$ compared to the DXA value

unknown, the aBMD derivation utilizes a technique which is influenced by the fat to lean ratio. This ratio computed as an average along the scan line or scan region of soft tissue close to the bone is dependent on the amount of red marrow, yellow marrow (equivalent to fat), and muscle present. Effectively, with more fat present, the smaller will be the apparent density. QCT is a multiple-projection acquisition technique not constrained by the above limitations; essentially, the aBMD of each pixel is greatly influenced by the linear attenuation coefficients derived during the reconstruction of the multiple projections acquired in a CT scan.

Next, the projected bone area used in the aBMD calculation was lower when produced by QCT than when produced by DXA analysis. This difference in projected area was observed at all sites, with the exception of the FN. There are several possible reasons for this. Firstly, the difference in projection geometry alludes to spatially dependent magnification with the fan beam geometry versus homogeneous magnification with the parallel beam geometry. Secondly, differences in noise properties of the QCT and DXA projection images comes about, in part, due to differences in the segmentation methods used. A DXA bone projection image is essentially a difference of two images with a residual noise component that extends throughout the bone projection image, including into regions outside of the bone. The noise properties of the QCT-derived bone projection image are much different to DXA because the soft tissue in which the bone is embedded is removed entirely from the image data prior to projection.

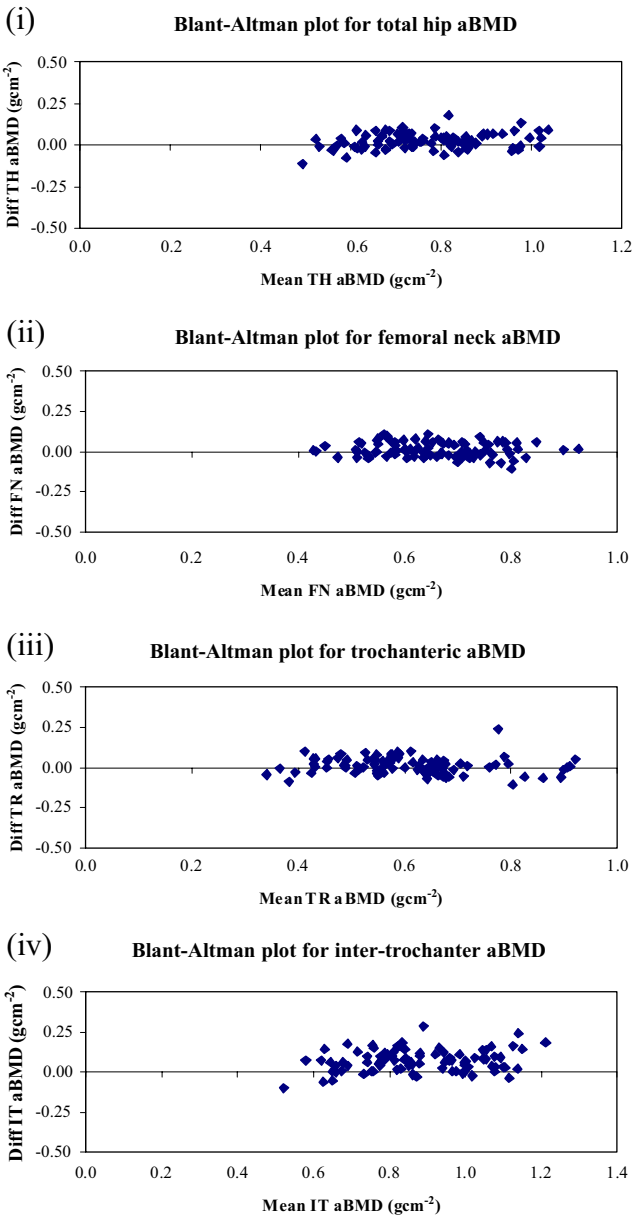

Fig. 2 Bland Altman plots showing absolute differences (DXA-derived aBMD–QCT_{DXA} aBMD) versus their mean for (*i*) total hip aBMD 0.02 (0.05) g cm^{-2} [mean (SD)], (*ii*) femoral neck 0.01 (0.04) g cm^{-2}, (*iii*) inter-trochanter 0.03 (0.07) g cm^{-2}, and (*iv*) trochanter 0.02 (0.05) g cm^{-2}. The trend was significant for IT ($p=0.03$) and TH ($p=0.03$)

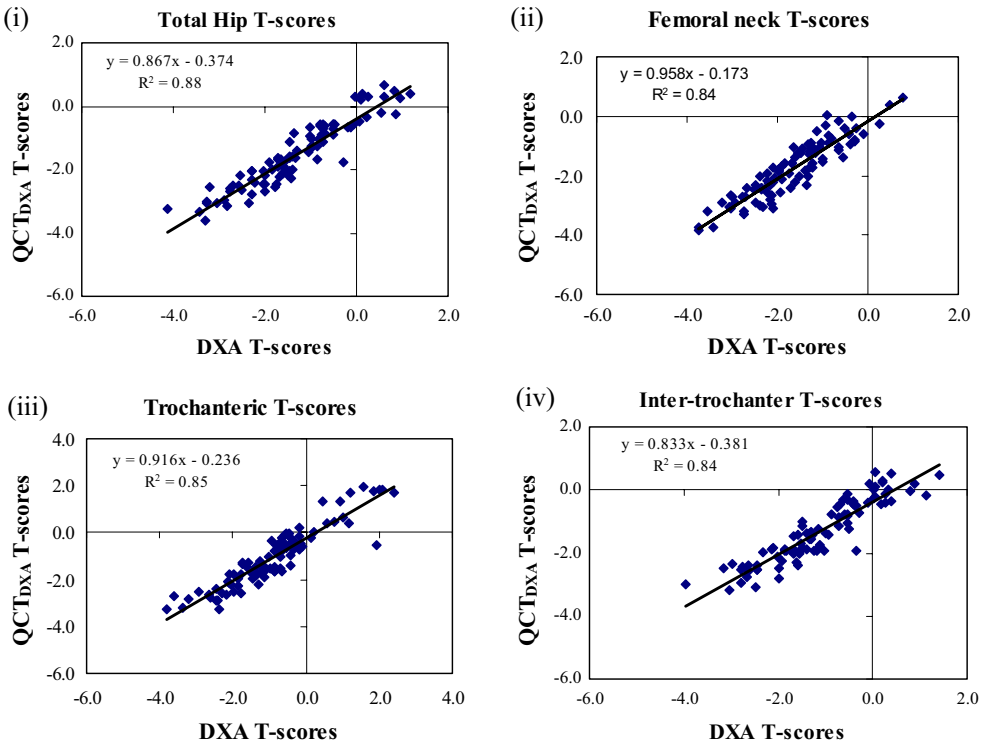

Fig. 3 Regression plots for QCT_{DXA} and DXA-derived aBMD *T* scores. (*i*), (*ii*), (*iii*), and (*iv*). The RMS error for TH, FN, IT, and TR were 0.36, 0.40, 0.39, and 0.49, respectively

A QCT projection image essentially goes zero just outside the bone with basically no noise. These differences in image noise properties are likely to influence algorithms used to estimate bone boundaries or projected areas. It is also possible that, even if identical algorithms were used, the performance of these algorithms may be influenced by the variation in noise properties of the projection images. The third factor relates to patient positioning, where the projection view generated by DXA may be different relative to the view generated by QCT. QCT analysis is performed such that the femoral neck axis, as viewed in three dimensions, is parallel to the plane of the projection image. DXA does not provide a measure of the femoral neck in three dimensions, and so the constraint of the physical (3D) femoral neck axis being parallel to the projection plane is neither assessed nor enforced in routine DXA study. So while the QCT and DXA projection planes are very similar, there may be a difference in the projection views that contributes to the observed difference in projected area.

As shown in this paper, it is possible to correct for the absolute differences between the two techniques because the differences are derived from the differing physical principle of the two techniques which are linear across the clinical range of interest reported in this study. A deficiency of this study is that it was only done in an elderly cohort of female osteoporotic subjects. It would be useful to perform a similar study spanning a wider age spread, both genders, and varying degrees of obesity, to test the regression equations in other groups.

The merit of a QCT study is that structural geometrical variables may be computed in addition to aBMD, for example, structural variables such as section modulus (Z) and cross-sectional area. These structural geometrical variables, demonstrated to be useful in the understanding of bone fragility, are also available from analysis of DXA hip images [14].

This study investigated associations between Hologic-based DXA and QCT, intentionally because the NHANES data were basically acquired using Hologic-based DXA systems. This study did not involve GE-Lunar DXA systems; thus, we have not provided associations between QCT and GE-Lunar-based DXA systems, but, as alluded to by way of aBMD offsets, it is apparent that Hologic-based DXA systems lies midway between QCT and GE-Lunar. Without the benefit of GE-Lunar analysis, it is anticipated that QCT and GE-Lunar associations will generally be similar to QCT and Hologic associations, with larger variations.

In conclusion, this study has shown a high correlation between DXA aBMD and QCT_{DXA} aBMD for the TH, FN, IT, and TR sites using vendor equipment, software, and regression equations. However, the QCT_{DXA} aBMD was systematically lower even after transformation to normalize *T* scores using the NHANES III reference data. Nevertheless, these offsets are small, can be corrected using the data provided in this paper, and in clinical practice are unlikely to substantially alter management. Thus, the use of QCT aBMD can be recommended to obtain NHANES-III-comparable values of *T* scores as well as offering the

prospect of detecting other abnormalities in femoral structure not detectable by DXA.

Conflicts of interest Dr. Brown and Dr. Cann are both stockholders of Mindways Software Inc.

Appendix

The TH QCT-derived aBMD may be converted to an equivalent TH DXA *T* score using the following relationships to facilitate application with WHO guidelines:

$$\mathrm{DXA}_{\mathrm{TH\_}T_{\mathrm{scores}}} = \mathrm{QCT}_{\mathrm{DXA\_TH\_}T_{\mathrm{scores}}} \times 1.15 + 0.43 \quad \ldots \quad (2)$$

or

$$\mathrm{DXA}_{\mathrm{TH\_}T_{\mathrm{scores}}} = \mathrm{QCT}_{\mathrm{TH\_aBMD}} \times 9.40 - 7.48 \quad \ldots \quad (3)$$

Where $\mathrm{QCT}_{\mathrm{DXA\_TH\_}T_{\mathrm{scores}}}$ is the NHANES III $\mathrm{QCT}_{\mathrm{DXA}}$ *T* score for the TH; $\mathrm{QCT}_{\mathrm{TH\_aBMD}}$ is the QCT-derived aBMD for the TH and $\mathrm{DXA}_{\mathrm{TH\_}T_{\mathrm{scores}}}$ is the equivalent DXA *T* score for the TH that may be applied to WHO *T* scores (for TH).

Similar relationships may also be derived for the FN:

$$\mathrm{DXA}_{\mathrm{FN\_}T_{\mathrm{scores}}} = \mathrm{QCT}_{\mathrm{DXA\_FN\_}T_{\mathrm{scores}}} \times 1.04 + 0.18 \quad \ldots \quad (4)$$

or

$$\mathrm{DXA}_{\mathrm{FN\_}T_{\mathrm{scores}}} = \mathrm{QCT}_{\mathrm{FN\_aBMD}} \times 10.59 - 7.76 \quad \ldots \quad (5)$$

inter-trochanter (IT):

$$\mathrm{DXA}_{\mathrm{IT\_}T_{\mathrm{scores}}} = \mathrm{QCT}_{\mathrm{DXA\_IT\_}T_{\mathrm{scores}}} \times 1.20 + 0.46 \quad \ldots \quad (6)$$

or

$$\mathrm{DXA}_{\mathrm{IT\_}T_{\mathrm{scores}}} = \mathrm{QCT}_{\mathrm{IT\_aBMD}} \times 7.79 - 7.17 \quad \ldots \quad (7)$$

and trochanter (TR):

$$\mathrm{DXA}_{\mathrm{TR\_}T_{\mathrm{scores}}} = \mathrm{QCT}_{\mathrm{DXA\_TR\_}T_{\mathrm{scores}}} \times 1.09 + 0.26 \quad \ldots \quad (8)$$

or

$$\mathrm{DXA}_{\mathrm{TR\_}T_{\mathrm{scores}}} = \mathrm{QCT}_{\mathrm{TR\_aBMD}} \times 10.97 - 6.51 \quad \ldots \quad (9)$$

References

1. Kanis JA, Gluer CC (2000) An update on the diagnosis and assessment of osteoporosis with densitometry. Committee of Scientific Advisors, International Osteoporosis Foundation. Osteoporosis Int 11:192–202
2. Tucker G, Metcalfe A, Pearce C et al (2007) The importance of calculating absolute rather than relative fracture risk. Bone 41 (6):937–941
3. Lang TF, Keyak JH, Heitz MW et al (1997) Volumetric quantitative computed tomography of the proximal femur: precision and relation to bone strength. Bone 21:101–108
4. Mayhew PM, Thomas CD, Clement JG et al (2005) Relation between age, femoral neck cortical stability, and hip fracture risk. Lancet 366(9480):129–135
5. Prince RL, Devine A, Dhaliwal SS et al (2006) Effects of calcium supplementation on clinical fracture and bone structure: results of a 5-year, double-blind, placebo-controlled trial in elderly women. Arch Intern Med 166(8):869–875
6. Cann CE, Genant HK (1980) Precise measurement of vertebral mineral content using computed tomography. J Comput Assist Tomogr 4:493–500
7. Khoo BCC (2006) Dosimetry assessment for QCT (hip and spine) and 3-D DXA (hip) for Human Rights Ethics Committee (HREC) submission. Internal Report of Department of Medical Technology and Physics, Sir Charles Gairdner Hospital, Nedlands
8. Looker AC, Orwoll ES, Johnston CC Jr et al (1997) Prevalence of low femoral bone density in older US adults from NHANES III. J Bone Miner Res 12:1761–1768
9. Henzell S, Dhaliwal S, Pontifex R et al (2000) Precision error of fan-beam dual X-ray absorptiometry scans at the spine, hip, and forearm. J Clin Densitom 3(4):359–364
10. Genant HK, Grampp S, Gluer CC et al (1994) Universal standardization for dual X-ray absorptiometry: patient and phantom cross-calibration results. J Bone Miner Res 9:1503–1514
11. Hui SL, Gao S, Zhou XH et al (1997) Universal standardization of bone density measurements: a method with optimal properties for calibration among several instruments. J Bone Miner Res 12:1463–1470
12. Sheperd JA, Fan B, Lu Y et al (2006) Comparison of BMD for prodigy and Delphi spine and femur scans. Osteoporosis Int 17:1303–1308
13. Goodsitt MM (1992) Conversion relations for quantitative CT bone mineral densities measured with solid and liquid calibration standards. Bone and Mineral 19:145–158
14. Nurzenski MK, Briffa NK, Price RI et al (2007) Geometric indices of bone strength are associated with physical activity and dietary calcium intake in healthy older women. J Bone Miner Res. 22(3):416–424